

# Increasing Risk of Wild Swings between Droughts and Floods over Global Land Areas

Linyin Cheng

University of Arkansas at Fayetteville

Zhiyong Liu (✉ [liuzhiy25@mail.sysu.edu.cn](mailto:liuzhiy25@mail.sysu.edu.cn))

Sun Yat-sen University <https://orcid.org/0000-0002-6930-5879>

Xiaohong Chen

Sun Yat-sen University

Kairong Lin

Sun Yat-sen University <https://orcid.org/0000-0001-6533-3357>

---

## Article

**Keywords:** dry-to-wet transition, anthropogenic climate change, global droughts, floods, risk

**Posted Date:** August 7th, 2020

**DOI:** <https://doi.org/10.21203/rs.3.rs-50300/v1>

**License:** © ⓘ This work is licensed under a Creative Commons Attribution 4.0 International License.

[Read Full License](#)

---

# **Increasing Risk of Wild Swings between Droughts and Floods over Global Land Areas**

## **Abstract**

**Climate variability is nothing new. Of rising concern is the consecutive occurrence of reversed weather patterns — droughts followed by severe floods, which tip a precarious balance with lasting impacts on human and natural systems. Here we examined changes in the likelihood and spatial distribution of dry-to-wet precipitation events over global land surface using climate model projections. We find anthropogenic climate change is likely to stress more widespread regions with rapid see-saw changes from dry to wet spells by the end of the 21<sup>st</sup> Century, increasing the threat to water security. Additionally, Eastern North America, South and East Asia, and Eastern Africa are emerging future hotspots of extreme drought-deluge swings by yielding marked enhancements in the events' occurrence probability and spatial coverage. This study can provide useful information for policy makers to develop integrated approach to drought and flood management, while broadening the scope of research on compound climate extremes.**

Keywords:

dry-to-wet transition, anthropogenic climate change, global droughts, floods, risk

1 Studies have warned us to expect more frequent and intense extreme events in the context of  
2 climate change<sup>1,2</sup>. With increasing frequency, many regions of the world have experienced wild  
3 weather patterns that swing from one extreme to another, dubbed as “weather whiplash” or  
4 “climate whiplash”<sup>3,4</sup>. While a certain amount of the swing is part of natural climate variability,  
5 what calls attention is the synchronicity of two contrasting extreme events such as droughts and  
6 floods. Floods are associated with extremes in rainfall, whereas drought is a protracted period of  
7 deficient precipitation<sup>5</sup>. From crippling droughts to deadly floods or vice versa, the rapid  
8 transition from one end of precipitation spectrum to the other concerns greater impacts than the  
9 sum of each individual type of event<sup>6</sup>. A dramatic example in this regard is the recent California.  
10 Immediately after multi-year dryness from 2012 to 2016, California, U.S. finds itself contending  
11 with the opposite: abundant precipitation and widespread flooding in the succeeding winter of  
12 2016–2017 that damaged hundreds of roads throughout the state and hastened the failure of the  
13 Oroville Dam’s primary spillway<sup>7</sup>.

14

15 Though droughts and floods have been widely studied at regional to continental scales<sup>8-11</sup>, it is  
16 typical to examine them individually. In the case of precipitation whiplash, droughts and floods  
17 are two sides of the same coin, spelling double trouble for agricultural yields, water quality, and  
18 human livelihood. Their successive occurrence, commingled with uneven population distribution  
19 and interconnected infrastructure systems could cause even more of a strain on nations’ ability to  
20 maintain the social, economic and environmental sustainability<sup>17-20</sup>. However, existing studies  
21 are few and have primarily focused on specific whiplash-like events at regional scale<sup>12-16</sup>. A  
22 global picture is lacking, except the recent study which explored the aggregated behavior of  
23 drought-pluvial seesaws over the globe from a historical perspective<sup>6</sup>. As the world warms,

24 abrupt shifts in weather patterns — droughts followed by severe floods — are conjectured to  
25 intensify<sup>21,22,23</sup>. The more connected relations between opposing precipitation extremes pose a  
26 different set of questions: What is the likelihood to anticipate heavy rainfall given a preceding  
27 dry spell? Where might be exposed to alternating effects of droughts and floods more probable  
28 than before? How likely the unusual shifts in precipitation similar or greater in magnitude to  
29 those that have historically caused widespread disruption would (re)occur in the future? Without  
30 this information, it is difficult to plan ahead for the potentially increased climate volatility<sup>17,24</sup>.

31  
32 Motivated by these questions, this study delivers a probabilistic assessment of dry-to-wet  
33 precipitation events at global scale using large ensembles of the Community Earth System Model  
34 (CESM) simulations and a conditional statistical approach. At each land grid, we define droughts  
35 and floods of future projections with respect to low and high percentiles of the historical  
36 precipitation climatology. Our objective is to estimate the probability of transitioning from a  
37 significant drought year to a following extreme wet year, characterize their spatial distributions,  
38 and quantify how these attributes may be altered as a consequence of human-induced climate  
39 change by the end of the 21<sup>st</sup> Century.

40

#### 41 **A Global Pattern for Extreme Dry-to-Wet Occurrence Likelihood**

42 As detailed in Method, we derived the probability of transitioning from extreme dry to wet states  
43 for four forty-year periods in Figure 1 and compared the results with previous studies. For  
44 instance, our framework identified a probability between 0.2~0.3 for which a dry spell is  
45 succeeded by heavy precipitation over the northern and southern part of the U.S. Great Plains in  
46 1960–2000. Similarly, Christian et al., 2015<sup>16</sup> concluded that there is about 25% chance that a

47 significant drought year is followed by a significant pluvial year within the Great Plains using  
48 land-based precipitation data from 1896 to 2013. Our model-based findings are quantitatively  
49 consistent with the observed evidence, confirming the validity of the applied framework.

50  
51 The regions of low to high probability for extreme dry-to-wet swings are shaded from light  
52 yellow to dark blue, illustrating that virtually no continent is absolutely immune to the threat of  
53 floods and droughts occurring together at the same location from a probabilistic view. Globally  
54 speaking, the likelihood of having sharp precipitation whiplash during the period of 1920–2000  
55 approaches 0.3 (Fig. 1a and 1b). That means, if a drought had occurred in the first year, there is  
56 about 30% chance that the second year would switch to a flood risk resulting from heavy rain on  
57 average of the globe of the 20<sup>th</sup> Century. The occurrence likelihoods of dry-to-wet transition  
58 events have been on the rise since the latter half of the 20<sup>th</sup> Century and are projected to continue  
59 to rise across a wide range of latitudes in the current century (Fig. 1c and 1d). At low latitudes, it  
60 is clear that the transition probability enhances over time in the Asian monsoon regions and  
61 exceeds 0.4 over South and Southeast Asia by the mid-21<sup>st</sup> Century. The higher-than-average  
62 likelihood suggests that these areas are likely to undergo dry-to-wet shifts at a greater frequency  
63 than the majority of the world of the past century, partially due to the large increase in total rain  
64 in climatologically wet regions of the tropics associated with the increased moisture source from  
65 the warmer Indian Ocean<sup>25</sup>. Rainfall is also moderately increased over the extratropics of both  
66 hemispheres poleward of 50° latitude in the CESM (Supplementary Figure S1-S2), consistent  
67 with projections from other Coupled Model Intercomparison Project Phase 5 models<sup>26</sup>. The  
68 excess rainfall can in turn contribute to raising the possibility of rapid reversals in precipitation at

69 high-latitude continents, e.g., Northwestern territories of Canada, Eastern Canada, Northern  
70 Europe, Western Siberia, and Eastern Russia in the result.  
71

72 Another increasing trend is present at the mid-latitude continental regions including Midwest and  
73 South-Central United States and Southeastern China. As shown, the Midwest and the Four  
74 Corners of the United States — where Colorado, Utah, New Mexico and Arizona meet deepen  
75 the color after 2020s, an indication of amplified risk of flip-flop in precipitation. In concordance,  
76 USGCRP, 2018 demonstrated that communities in the Four Corners have been bouncing  
77 between desperate dryness and extreme moisture since the winter of 2017, forcing people  
78 dependent on the reliability and predictability of water to adapt<sup>27</sup>. While Midwest and South-  
79 Central United States are no strangers to drought-to-deluge oscillations, the concern is that more  
80 frequent vacillating weather conditions could change the storage of nutrients in the agricultural  
81 landscape and degrade the regions' quality of water supplies, pressing municipalities to seek  
82 costly remedies to provide residents with safe drinking water<sup>28</sup>. Enhanced likelihood is projected  
83 likewise for Arabian Gulf area, but absent for the southern Europe–Turkey region. In the  
84 midlatitudes, synoptic storms bring moist air from the ocean to the land, and sometimes they can  
85 account for more than 70% of a region's total precipitation<sup>29</sup>. The observed enhancement may  
86 have a link with changes in the storm tracks in a sense that pronounced storm track activity  
87 favors monthly rainfall extremes throughout the year, whereas dry spells are associated with a  
88 lack thereof<sup>30</sup>. Over Southern China, especially in the mid- and lower reaches of the Yangtze  
89 River valley, the elevated likelihood of drought-pluvial seesaws can be of a close relationship  
90 with the advance and retreat of the East Asian summer monsoon<sup>31</sup>.  
91

92 In the Southern Hemisphere, South America unfolds a contrasting pattern which persists from  
93 the past into the future. More explicitly, the territory is less frequently influenced by dry-wet  
94 dipole events over the northern South America and eastern Amazonia–Northeast Brazil region,  
95 while bearing a greater risk over Southwest and Southeast South America, involving Brazil,  
96 Bolivia, Paraguay, and Argentina. An analysis of precipitation climatology over the four periods  
97 reveals that precipitation is reduced over the broad Amazon and increased over the La Plata  
98 basin and central Argentina. Combining with the physical drivers that involve local soil-moisture  
99 feedbacks prevalent over the Amazon basin and remote effects of sea surface temperature over  
100 the Niño 3.4 region on the La Plata Basin, this dipolar response could be explained<sup>32</sup>.  
101 Additionally, we find Southern Africa and the northern Central Africa favor similar shifts in  
102 these low frequency weather patterns, potentially related to the seasonal movement of the  
103 Intertropical Convergence Zone. This finding is in line with He and Sheffield, 2020<sup>6</sup>, although  
104 their study focuses on the interannual precipitation variability of the recent past.

105

### 106 **Large Increase in the Global Land Areas Susceptible to Extreme Dry-to-Wet Events**

107 To quantify changes in the risk of precipitation whiplash, we assessed the percentage of global  
108 land areas subject to different levels of dry-to-wet transition probabilities in Figure 2. According  
109 to the 1920–1960 histogram (Fig. 2a), more than half of the land is designated with a likelihood  
110 less than 30%; only about 0.4% of the land surface yields a probability greater than 50%. In  
111 other words, during two consecutive years, 0.4% of the land may expect an extreme wet spell  
112 with more than 50% chance, viz., more likely in the year subsequent to the year of extreme  
113 dryness, yet the majority of the world would get flooding rain with a less than 30% chance in the  
114 following year during the period without appreciable human-induced climate change. Land areas

115 associated with higher probabilities expand a little in the next 40 years. The histogram of Fig. 2b  
116 shows that the percentage of land coverage grows from 0.4% to 2.6% at a probability above 0.5,  
117 implying that 2.6% of the global land is more likely to have suffered from severe floods and  
118 droughts in consecutive years by the end of the 20<sup>th</sup> Century. Even though, locations with a  
119 likelihood higher than 0.5 are scarce, and a probability greater than 0.6 is virtually non-existent,  
120 reflecting relatively low risks of extreme flux in precipitation for the twentieth-Century world.

121  
122 Looking ahead, dry-to-wet precipitation events are projected to occur at increased spatial  
123 coverage under transition probabilities above the global average (Fig. 2c and 2d), albeit the  
124 increase is slightly reduced in 2060–2100 in response to a tempered upward trend in  
125 precipitation. Approximate 9.3% and 4.3% of the spatial areas are found with transition  
126 probabilities of 0.5~0.6 and 0.6 beyond, respectively by the mid-21<sup>st</sup> Century, in contrast to 2.3%  
127 and 0.3% of the land in 1960–2000 considering the same probability levels. That is to say about  
128 13.6% of the land might see a drought year followed by an extreme wet year at more than 50%  
129 chance, quintupling the figure in the past century. Alternatively, land areas with lower  
130 occurrence probabilities of abrupt changes in precipitation are reduced, compensating for the  
131 increase in locations having larger odds. We report there is an appreciable increase in the  
132 percentage of land areas associated with a probability exceeding the 20<sup>th</sup> Century's global  
133 average — additional 10% of the territories are likely to be depressed by the year-to-year swings  
134 from droughts to floods in the current century, despite no material difference in the annual mean  
135 precipitation over the global land regions. Such shifts can bring more frequent and intense water  
136 cycle extremes to a broader landscape, posing a new challenge to the management of already  
137 declining freshwater resources.

138

139 To identify regional contributions to the global increase, we aggregated the land points into 21  
140 regions (Fig. 3a), largely consistent with the divisions used for examining global precipitation  
141 projections<sup>33</sup>. Through the bar chart analysis (Fig. 3b-e), we find the dry-to-wet precipitation  
142 events are likely to bear upon more than 70% of the Eastern North America (E.N.A) grids at the  
143 probabilities surpassing the global average, whereof more than 20% is likely to be affected at a  
144 greater-than-0.5 probability by the end of this century. The CESM projections show that it is  
145 becoming wetter in the eastern parts of North America (Supplementary Figure S1-S2), in part,  
146 because higher temperatures increase water-holding capacity and more precipitation falls as rain  
147 instead of snow<sup>5</sup>. With roughly 30% enlargement since the last century, the E.N.A manages to be  
148 one of the major contributors to the marked increase in land areas that are prone to whiplash of  
149 droughts and floods. Following the E.N.A are East Asia (E.As) and Eastern Africa (E.Af),  
150 subject to an analogous amount of increase with the probability beyond 0.3, and about twofold of  
151 increase when it reaches a more probable level of 0.5. Western Africa (W.Af), South Asia  
152 (S.As), Alaska (ASK) and Greenland (GLD) are projected to increase more than 20%,  
153 positioning among the top major contributors. On the contrary, a tendency towards a reduction of  
154 the drought-to-flood prone areas appears over Amazon Basin (AMZ), Central America (C.A),  
155 and Mediterranean (Med). The changes over Med could be connected to the increased  
156 anticyclonic circulation that yields increasingly stable conditions and is associated with a  
157 northward shift of the Atlantic storm track<sup>34</sup>.

158

159 **Regional Changes in the Likelihood of Extreme Dry-to-Wet Events**

160 Figure 4 collects the dry-to-wet transition probability at each grid of the 21 land regions in a box-  
161 whisker plot to identify future hotspots of precipitation whiplash. We examined whether the  
162 difference between each of the two periods is statistically significant based on the Student *t*-test.  
163 The symbols above the boxplots notify the testing results — from one to four stars, it  
164 corresponds to significant levels of 0.05, 0.01, 0.001, and 0.0001 respectively, and ns indicates  
165 non-significant. In the first place, the box-whisker plots disclose a spatial heterogeneity with  
166 variations in the direction and magnitude of transition probabilities over space. The spatial  
167 heterogeneity may stem from different climate change impacts on micro- and macro-scale  
168 atmospheric processes controlling extreme precipitation formation in different regions, a key  
169 interpretation of studies on climate change impact on extreme precipitation in the future  
170 projections<sup>35</sup>. Nonetheless, we note statistically significant upward trends with dry-to-wet  
171 transition probability well beyond the global average for all the four periods over regions,  
172 including E.N.A, E.Af, S.As, North Asia (N.As) and E.As. The increasing trends in Central Asia  
173 (C.Asia), Southern South America (S.SA) and W.Af are significant for the first three 40 years  
174 while milder for the last period. With the rising trends, these regions may exhibit an increased  
175 propensity for drought-flood seesaws, consistent with our previous findings. Western North  
176 America (W.N.A) and Central North America (C.N.A)’s upward trends are less significant,  
177 owing to, in part, the large variability in spatial distributions of the extreme dry-to-wet  
178 precipitation events, whereas no clear trend is detected in the rest regions.

179

180 Excluding the climatologically dry regions such as Alaska, Greenland and North Asia, the most  
181 prominent hotspot emerging from the box-whisker plots is the E.N.A. On the one hand, a  
182 significant increase in the dry-to-wet transition probability since the 1920 vintage typifies the

183 E.N.A region; on the other hand, it shows the highest likelihood among the 21 regions in the  
184 current century. Other emerging hotspots include S.As, E.As, and E.Af, due to the relatively high  
185 transition probability with distinguishable increments over the study periods. Demographic  
186 growth and shifts to such whiplash-prone locations can raise the number of human beings  
187 exposed. Plus the detected increase in vulnerable land areas, a variety of natural resources could  
188 be at risks in the 21<sup>st</sup> Century, and a paradigm shift from disaster relief to prevention will be  
189 crucial for buffering the worst effects of rapid transitions between extreme precipitation and the  
190 opposite.

191

## 192 **Research Implications**

193 Collectively, we find the percentage of global land areas susceptible to dry-to-wet transition  
194 events has been appreciably enhanced in the 21<sup>st</sup> Century, principally due to the human-induced  
195 climate change. In addition, the anthropogenic forcings are likely to heighten the likelihood of  
196 unusual shifts in precipitation over the global land surface, while inducing disproportionate  
197 impacts at regional scales. Potential future hotspots include Eastern North America, South and  
198 East Asia, and Eastern Africa, where the increasing greenhouse emissions can yield more  
199 frequent and widespread drought-deluge fluctuations with marked enhancement in the events'  
200 occurrence probability and spatial coverage in the current century.

201

202 A warmer atmosphere is associated with a greater water-holding capacity, whose role is likely to  
203 strengthen the global hydrological cycle<sup>36,37,38</sup>. Enhancement in the seasonal precipitation cycle  
204 would have notable consequences such that precipitation tends to be concentrated into more  
205 intense events, with longer periods of little precipitation in between<sup>39,40</sup>. As a result, deluge can

206 be interspersed with very dry interludes. Local changes in the character of precipitation relevant  
207 to the wild swings between droughts and floods depend upon a multitude of factors, involving  
208 large-scale atmosphere circulation and topographical conditions<sup>13,14,15,16,24,25</sup>; other influences  
209 from land–atmosphere feedback and a warming Arctic with loss of sea ice are also possible and  
210 remain a subject of ongoing research<sup>17,18</sup>. By probing changes in the likelihood and spatial  
211 distribution of dry-to-wet precipitation events, this study is expected to shed light on  
212 understanding the underlying mechanisms of drought-flood cycles and provide useful  
213 information for policy makers and infrastructure operators to develop integrated approach to  
214 drought and flood management. It is also worth noting that the proposed approach is broadly  
215 transferable and can be extended to tackle other scientific challenges related to abrupt changes in  
216 climate.

217  
218 While humans have long adapted to regimes of water scarcity or excess, we are vastly  
219 underprepared for climate extreme events, such as the “mega” droughts, unprecedented wildfires,  
220 or their combinations, also known as compound events<sup>41,42</sup>. According to the Intergovernmental  
221 Panel on Climate Change report, compound events describe multiple climate drivers and/or  
222 hazards that occur simultaneously or successively to contribute to societal or environmental  
223 risk<sup>41</sup>. In combination, these hazards caused devastating impacts well beyond that which any one  
224 of these hazards would have caused in isolation<sup>44</sup>, and for this reason, compound events have  
225 received increasing attention in the recent decade<sup>45,46,47,48,49</sup>. By definition, the consecutive  
226 occurrence of reversed weather patterns can be considered compound events; however,  
227 comparing to the concurrent climate extremes, e.g., droughts and heat waves, heavy precipitation  
228 and storm surge, etc., synchronicity of contrasting extreme events has been largely overlooked.

229 This study aims to broaden the scope of research on compound events by calling attention to  
230 climate whiplash, in particular, the rapid see-saw changes from dry to wet spells, which may  
231 seem rare but are likely to occur more frequently with severe consequences — disrupting plant  
232 growth, jeopardizing agricultural yields, and threatening the durability and longevity of  
233 buildings, all in much quicker cycles than one would typically plan for in the near future.

234

## 235 **Method**

### 236 **Project Data**

237 The monthly precipitation data is from the National Center for Atmospheric Research's single-  
238 model 'Large Ensemble Community Project' (LENS). We obtained 37 simulations of the  
239 Community Earth System Model (CESM) at  $1^\circ \times 1^\circ$  spatial resolution  
240 (<http://cesm.ucar.edu/projects/community-projects/LENS/>) for the period of 1920-2100. The  
241 future climate is simulated assuming the representative concentration pathway 8.5, i.e., RCP8.5  
242 scenario, in which greenhouse gas emissions continue to increase throughout the twenty-first  
243 century<sup>50</sup>. This is an extreme scenario, and so our results are borne with the caveat that, for lower  
244 emissions scenarios, changes might be less than presented in this study. Each ensemble member  
245 has distinct initial conditions, so that the difference between the members is due to internal  
246 variability and the ensemble mean is an estimate of the response to external forcing. Here we  
247 derived the statistics of extreme dry-to-wet events based on the CESM ensemble mean  
248 precipitation, changes of which are mainly caused by the human-induced climate change.

249

### 250 **Defining Dry-to-Wet Events**

251 For the purpose of this study, period from 1920 to 1960 is used as the baseline to derive  
252 anomalies of precipitation which limits factors in recent changes in climate. Using these  
253 precipitation anomalies, we identify dry and wet events for four forty-year periods, including  
254 1920-1960, 1960-2000, 2020-2060, and 2060-2100. Herein the dry-to-wet transition events are  
255 defined as the occurrence of two consecutive years during which the annual total precipitation  
256 falls under the 30<sup>th</sup> percentile of the baseline climatology (in the first year) and subsequently  
257 exceeds the 70<sup>th</sup> percentile of the same reference (in the following year). We have examined  
258 different thresholds, i.e., 20<sup>th</sup> and 80<sup>th</sup> percentiles of the baseline climatology. No material  
259 difference is observed from the current results in terms of the spatial distribution and transition  
260 probability of the dry-to-wet events, suggesting that the current finding is robust and independent  
261 of the given thresholds (Supplementary Figure S3). For both historical simulations (1920-1960  
262 and 1960-2000) and future projections (2020-2060 and 2060-2100), we assessed the occurrence  
263 probability of dry-to-wet transition events in each model run, based on which the upper and  
264 lower uncertainty range arising from the internal variability of the CESM simulations is derived  
265 (Supplementary Figures S4).

266

### 267 **Estimating the Probability of Dry-to-Wet Precipitation Events**

268 Yue and Rasmussen, 2002<sup>51</sup> gave a thorough review about how to obtain information concerning  
269 the occurrence probabilities of one variable under different conditions. Briefly, let  $f(x, y)$  be the  
270 joint probability density function (PDF) of two continuous random variables  $X$  and  $Y$ ,  $f_X(x)$  and  
271  $f_Y(y)$  be the marginal PDFs of  $X$  and  $Y$ , respectively, and  $F_X(x)$ ,  $F_Y(y)$ , and  $F(x, y)$  be the  
272 corresponding Cumulative Distribution Functions (CDFs) for their univariate and bivariate  
273 variables. The conditional PDF of  $X$  given  $Y = y$  can be expressed as:

274 
$$f_{X|Y}(x|y) = \frac{f(x,y)}{f_Y(y)} \quad (1)$$

275 Based on the PDF, the conditional CDF of  $X$  given  $Y = y$  is derived as:

276 
$$F_{X|Y} = \int_{-\infty}^x f_{X|Y}(u|y) du = \frac{\int_{-\infty}^x f(u,y) du}{f_Y(y)} \quad (2)$$

277 Similarly, the conditional CDF of  $X \leq x$  given  $Y \leq y$  has the following expression:

278 
$$F'_{X|Y}(x|y) = F(x|Y \leq y) = \frac{F(x,y)}{F_Y(y)} \quad (3)$$

279 The exceeding probability of Equation (3) is a measure of the likelihood associated with the  
 280 event  $X > x$  given  $Y \leq y$ , which is formulated as<sup>52</sup>:

281 
$$P_{X>x|Y\leq y} = 1 - F(x|Y \leq y) = 1 - \frac{F(x,y)}{F_Y(y)} \quad (4)$$

282 If an extremely dry event has occurred in the first year, the interest is to estimate how likely the  
 283 following year would be subject to the opposite scenario of extreme wetness. Essentially, that is  
 284 the probability of  $X$  conditioned upon  $Y$ , i.e.,  $P(X > x|Y \leq y)$ , where  $x$  and  $y$  represent the  
 285 thresholds for defining the wet and dry states, respectively. This conditional probability conveys  
 286 the likelihood of a subsequent flood year occurring given that a prior drought year has  
 287 occurred<sup>53</sup>. It can also be interpreted as the probability of transitioning from one state to another  
 288 (herein dry to wet states) in a single step, broadly known as the one-step transition probability<sup>54</sup>.

289 The key to solving Equation (4) relies on the construction of the joint distribution between  $X$   
 290 and  $Y$ . In this study, we employed the bivariate copula which allows for joining the margins and  
 291 modeling the joint dependence structure between extreme wet and dry states of precipitation.

292

293 Unlike multivariate distribution functions, such as the bivariate Gaussian or Gamma  
 294 distributions, copulas do not require all of the marginal distributions to come from the same

295 distribution<sup>52</sup>. Copula functions are defined as multivariate distribution functions with uniformly  
296 distributed variables on the interval [0, 1]<sup>55</sup>:

$$297 \quad F(x_1, \dots, x_i, \dots, x_n) = C(F(x_1), \dots, F(x_i), \dots, F(x_n)) = C(u_1, \dots, u_i, \dots, u_n) \quad (5)$$

298 where  $C$  is the CDF of the copula, and  $F(x_i)$  is the marginal distribution of  $x_i$  being uniform on  
299 the interval [0, 1], which is also denoted by  $u_i$ . Note that  $C$  connects the CDFs of the random  
300 variables (i.e.,  $u_i$ ), whereas  $F(x_1, \dots, x_n)$  in the left-hand side represents the joint probability of  
301 the original random variables (i.e.,  $x_i$ ). Let  $U = F(y)$  and  $V = F(x)$ ; and  $u$  will denote a specific  
302 value of  $U$  and  $v$  will denote a specific value of  $V$ . Substituting the bivariate copula for  $x$  and  $y$ ,  
303 into Equation (4), it becomes:

$$304 \quad P_{X>x|Y\leq y} = 1 - C(u, v)/u \quad (6)$$

305 Equation (6) thus refers to the probability of transitioning from a significant dry year to a  
306 following extreme wet year, or equivalently, the occurrence likelihood of a whiplash event of  
307 drought and floods. Different copulas are available for the joint analysis of precipitation  
308 extremes. Here we examined six widely applied bivariate copulas, including Gaussian, Student t,  
309 Gumbel, Joe, Frank and Clayton at each grid of the study domain. The goodness-of-fit of copula  
310 is tested using the Akaike information criterion<sup>56</sup>; and the parameters of copula functions were  
311 derived using the method of maximum likelihood estimation<sup>57</sup>.

312

313

314

315

316

317

318

319

320 **References**

- 321 1. Coumou, D. & Rahmstorf, S. A decade of weather extremes. *Nature climate change* **2**, 491-  
322 496 (2012).
- 323 2. Diffenbaugh, N.S., et al. Quantifying the influence of global warming on unprecedented  
324 extreme climate events. *Proceedings of the National Academy of Sciences* **114**, 4881-4886  
325 (2017).
- 326 3. Cappucci, M. The Washington Post (2020).
- 327 4. Freedman, A. The Washington Post (2009).
- 328 5. Trenberth, K.E. *Encyclopedia of hydrological sciences Part 17. Climate Change* (John Wiley  
329 & Sons, Ltd, Hoboken, 2005).
- 330 6. He, X. & Sheffield, J. Lagged compound occurrence of droughts and pluvials globally over  
331 the past seven decades. Preprint at <https://doi.org/10.1029/2020GL087924> (2020).
- 332 7. Wang, S.Y.S., Yoon, J.H., Becker, E. & Gillies, R. California from drought to deluge. *Nature*  
333 *Climate Change* **7**, 465 (2017).
- 334 8. Trenberth, K.E., et al. Global warming and changes in drought. *Nature Climate Change* **4**,  
335 17-22 (2014).
- 336 9. Dai, A. Increasing drought under global warming in observations and models. *Nature climate*  
337 *change* **3**, 52-58 (2013).
- 338 10. Hirabayashi, Y., et al. Global flood risk under climate change. *Nature Climate Change* **3**,  
339 816-821 (2013).
- 340 11. Milly, P.C.D., Wetherald, R.T., Dunne, K.A. & Delworth, T.L. Increasing risk of great floods  
341 in a changing climate. *Nature* **415**, 514-517 (2002).
- 342 12. Calvin, W.H. *A brain for all seasons: Human evolution and abrupt climate change*.  
343 (University of Chicago Press, Chicago, 2002).
- 344 13. Dong, X., et al. Investigation of the 2006 drought and 2007 flood extremes at the Southern  
345 Great Plains through an integrative analysis of observations. *Journal of Geophysical*  
346 *Research: Atmospheres* **116**, D3 (2011).
- 347 14. Seager, R., Pederson, N., Kushnir, Y., Nakamura, J. & Jurburg, S. The 1960s drought and the  
348 subsequent shift to a wetter climate in the Catskill Mountains region of the New York City  
349 watershed. *Journal of Climate* **25**, 6721-6742 (2012).
- 350 15. Parry, S., Marsh, T. & Kendon, M. 2012: from drought to floods in England and  
351 Wales. *Weather* **68**, 268-274 (2013).
- 352 16. Christian, J., Christian, K. & Basara, J.B. Drought and pluvial dipole events within the great  
353 plains of the United States. *Journal of Applied Meteorology and Climatology* **54**, 1886-1898  
354 (2015).
- 355 17. Swain, D.L., Langenbrunner, B., Neelin, J.D. & Hall, A. Increasing precipitation volatility in  
356 twenty-first-century California. *Nature Climate Change* **8**, 427-433 (2018).
- 357 18. Casson, N.J., et al. Winter weather whiplash: impacts of meteorological events misaligned  
358 with natural and human systems in seasonally snow-covered regions. *Earth's Future* **7**, 1434-  
359 1450 (2019).

- 360 19. De Sherbinin, A., Schiller, A. & Pulsipher, A. The vulnerability of global cities to climate  
361 hazards. *Environment and urbanization* **19**, 39-64 (2007).
- 362 20. Roaf, S., Roaf, S., Crichton, D. & Nicol, F. *Adapting buildings and cities for climate change:  
363 a 21st century survival guide*. (Routledge, London, 2009).
- 364 21. Steffensen, J.P., et al. High-resolution Greenland ice core data show abrupt climate change  
365 happens in few years. *Science* **321**, 680-684 (2008).
- 366 22. Yoon, J.H., et al. Increasing water cycle extremes in California and in relation to ENSO cycle  
367 under global warming. *Nature Communications* **6**, 1-6 (2015).
- 368 23. Prein, A.F., et al. The future intensification of hourly precipitation extremes. *Nature Climate  
369 Change* **7**, 48-52 (2017).
- 370 24. Trouet, V., Babst, F. & Meko, M. Recent enhanced high-summer North Atlantic Jet  
371 variability emerges from three-century context. *Nature communications* **9**, 1-9 (2018).
- 372 25. Meehl, G.A. & Arblaster, J.M. Mechanisms for projected future changes in south Asian  
373 monsoon precipitation. *Climate Dynamics* **21**, 659-675 (2003).
- 374 26. Lau, W.K.M., Wu, H.T. & Kim, K.M. A canonical response of precipitation characteristics to  
375 global warming from CMIP5 models. *Geophysical Research Letters* **40**, 3163-3169 (2013).
- 376 27. Reidmiller D.R., et al. *Fourth national climate assessment. Volume II: Impacts, Risks, and  
377 Adaptation in the United States, Report-in-Brief*. (Washington, DC: US Global Change  
378 Research Program, 2018).
- 379 28. Loecke, T.D., et al. Weather whiplash in agricultural regions drives deterioration of water  
380 quality. *Biogeochemistry* **133**, 7-15 (2017).
- 381 29. Hawcroft, M.K., Shaffrey, L.C., Hodges, K.I. & Dacre, H.F. How much Northern  
382 Hemisphere precipitation is associated with extratropical cyclones?. *Geophysical Research  
383 Letters* **39**, 24 (2012).
- 384 30. Lehmann, J. & Coumou, D. The influence of mid-latitude storm tracks on hot, cold, dry and  
385 wet extremes. *Scientific reports* **5**, 17491 (2015).
- 386 31. Wu, Z., Li, J., He, J. & Jiang, Z. Occurrence of droughts and floods during the normal  
387 summer monsoons in the mid-and lower reaches of the Yangtze River. *Geophysical Research  
388 Letters* **33**, 5 (2006).
- 389 32. Llopart, M., Coppola, E., Giorgi, F., Da Rocha, R.P. & Cuadra, S.V. Climate change impact  
390 on precipitation for the Amazon and La Plata basins. *Climatic Change* **125**, 111-125 (2014).
- 391 33. Giorgi, F. & Bi, X. Updated regional precipitation and temperature changes for the 21st  
392 century from ensembles of recent AOGCM simulations. *Geophysical Research Letters* **32**, 21  
393 (2005).
- 394 34. Giorgi, F. & Lionello, P. Climate change projections for the Mediterranean region. *Global  
395 and planetary change* **63**, 90-104 (2008).
- 396 35. Fischer, E.M. & Knutti, R. Anthropogenic contribution to global occurrence of heavy-  
397 precipitation and high-temperature extremes. *Nature Climate Change* **5**, 560-564 (2015).
- 398 36. Huntington, T.G. Evidence for intensification of the global water cycle: review and  
399 synthesis. *Journal of Hydrology* **319**, 83-95 (2006).
- 400 37. Held, I.M. & Soden, B.J. Robust responses of the hydrological cycle to global  
401 warming. *Journal of climate* **19**, 5686-5699 (2006).
- 402 38. Wentz, F.J., Ricciardulli, L., Hilburn, K. & Mears, C. How much more rain will global  
403 warming bring?. *Science* **317**, 233-235 (2007).
- 404 39. Seager, R., Naik, N. & Vogel, L. Does global warming cause intensified interannual  
405 hydroclimate variability?. *Journal of Climate* **25**, 3355-3372 (2012).

- 406 40. Chou, C., et al. Increase in the range between wet and dry season precipitation. *Nature*  
407 *Geoscience* **6**, 263-267 (2013).
- 408 41. Leonard, M., et al. A compound event framework for understanding extreme impacts. *Wiley*  
409 *Interdisciplinary Reviews: Climate Change* **5**, 113-128 (2014).
- 410 42. AghaKouchak, A., et al. Climate Extremes and Compound Hazards in a Warming  
411 World. *Annual Review of Earth and Planetary Sciences* **48**, 519-548 (2020).
- 412 43. Field, C.B., Barros, V., Stocker, T.F. & Dahe, Q. eds. *Managing the risks of extreme events*  
413 *and disasters to advance climate change adaptation: special report of the intergovernmental*  
414 *panel on climate change* (Cambridge University Press, Cambridge, 2012).
- 415 44. Zscheischler, J., et al. Future climate risk from compound events. *Nature Climate Change* **8**,  
416 469-477 (2018).
- 417 45. Zscheischler J, & Seneviratne SI. Dependence of drivers affects risks associated with  
418 compound events. *Science advances* **3**, 6 (2017).
- 419 46. Cheng, L., et al. How has human-induced climate change affected California drought  
420 risk?. *Journal of Climate* **29**, 111-120 (2016).
- 421 47. Bevacqua, E., et al. Higher probability of compound flooding from precipitation and storm  
422 surge in Europe under anthropogenic climate change. *Science advances* **5**, 5531 (2019).
- 423 48. Wahl, T., Jain, S., Bender, J., Meyers, S.D. & Luther, M.E., 2015. Increasing risk of  
424 compound flooding from storm surge and rainfall for major US cities. *Nature Climate*  
425 *Change* **5**, 1093-1097.
- 426 49. Hao, Z., Hao, F., Xia, Y., Singh, V.P. & Zhang, X., 2019. A monitoring and prediction  
427 system for compound dry and hot events. *Environmental Research Letters* **14**, 114034.
- 428 50. Kay, J.E., et al. The Community Earth System Model (CESM) large ensemble project: A  
429 community resource for studying climate change in the presence of internal climate  
430 variability. *Bulletin of the American Meteorological Society* **96**, 1333-1349 (2015).
- 431 51. Yue, S. & Rasmussen, P. Bivariate frequency analysis: discussion of some useful concepts in  
432 hydrological application. *Hydrological Processes* **16**, 2881-2898 (2002).
- 433 52. Cheng, L., Hoerling, M., Smith, L. & Eischeid, J. Diagnosing human-induced dynamic and  
434 thermodynamic drivers of extreme rainfall. *Journal of Climate* **31**, 1029-1051 (2018).
- 435 53. Anderson, T.W. & Goodman, L.A. Statistical inference about Markov chains. *The Annals of*  
436 *Mathematical Statistics* **28**, 89-110 (1957).
- 437 54. Salvadori, G. & De Michele, C. Frequency analysis via copulas: Theoretical aspects and  
438 applications to hydrological events. *Water resources research* **40**, 12 (2004).
- 439 55. Joe, H. *Multivariate models and multivariate dependence concepts* (CRC Press, Cleveland,  
440 1997).
- 441 56. Liu, Z. et al. A framework for exploring joint effects of conditional factors on compound  
442 floods. *Water Resources Research* **54**, 2681-2696 (2018).
- 443 57. Kojadinovic, I. & Yan, J., 2010. Modeling multivariate distributions with continuous margins  
444 using the copula R package. *Journal of Statistical Software* **34**, 1-20 (2010).

445

446

447

448

449 **Figure Legends**

450 Figure 1. The probability of dry-to-wet precipitation events for four forty-year periods including  
451 1920-1960 (a), 1960-2000 (b), 2020-2060 (c) and 2060-2100 (d). The dry-to-wet transition  
452 events are defined as the occurrence of two consecutive years during which the annual total  
453 precipitation falls under the 30<sup>th</sup> percentile of the baseline climatology (in the first year) and  
454 subsequently exceeds the 70<sup>th</sup> percentile of the same reference (in the following year).

455

456 Figure 2. The percentage of global land areas subject to different levels of dry-to-wet transition  
457 probabilities for 1920-1960 (a), 1960-2000 (b), 2020-2060 (c) and 2060-2100 (d).

458

459 Figure 3. The percentage of global land areas subject to different levels of dry-to-wet transition  
460 probabilities for 21 subregions (a) during periods of 1920-1960 (b), 1960-2000 (c), 2020-2060  
461 (c) and 2060-2100 (e).

462

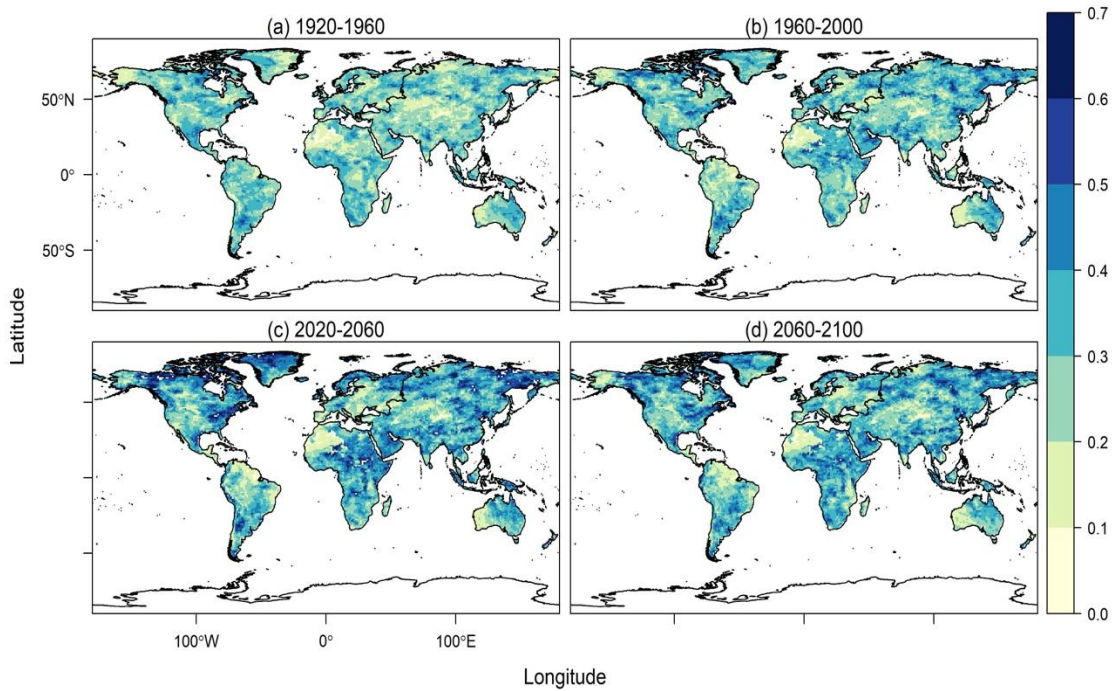
463 Figure 4. The probability of transitioning from a significant drought year to a following extreme  
464 wet year during each of the four forty-year periods for the 21 subregions. A, B, C and D  
465 correspond to the periods of 1920-1960, 1960-2000, 2020-2060 and 2060-2100, respectively.

466

467

468

469

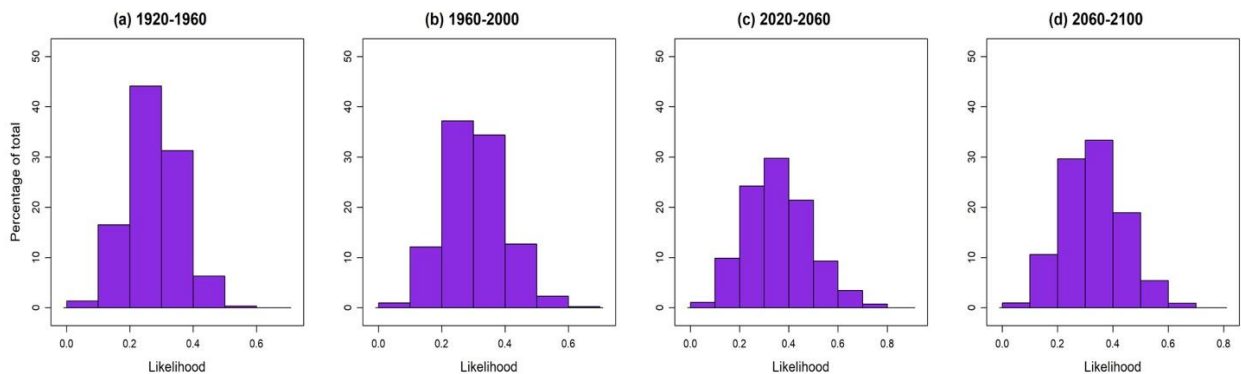


470

471 Figure 1. The probability of dry-to-wet precipitation events for four forty-year periods including  
 472 1920-1960 (a), 1960-2000 (b), 2020-2060 (c) and 2060-2100 (d). The dry-to-wet transition  
 473 events are defined as the occurrence of two consecutive years during which the annual total  
 474 precipitation falls under the 30th percentile of the baseline climatology (in the first year) and  
 475 subsequently exceeds the 70th percentile of the same reference (in the following year).

476

477



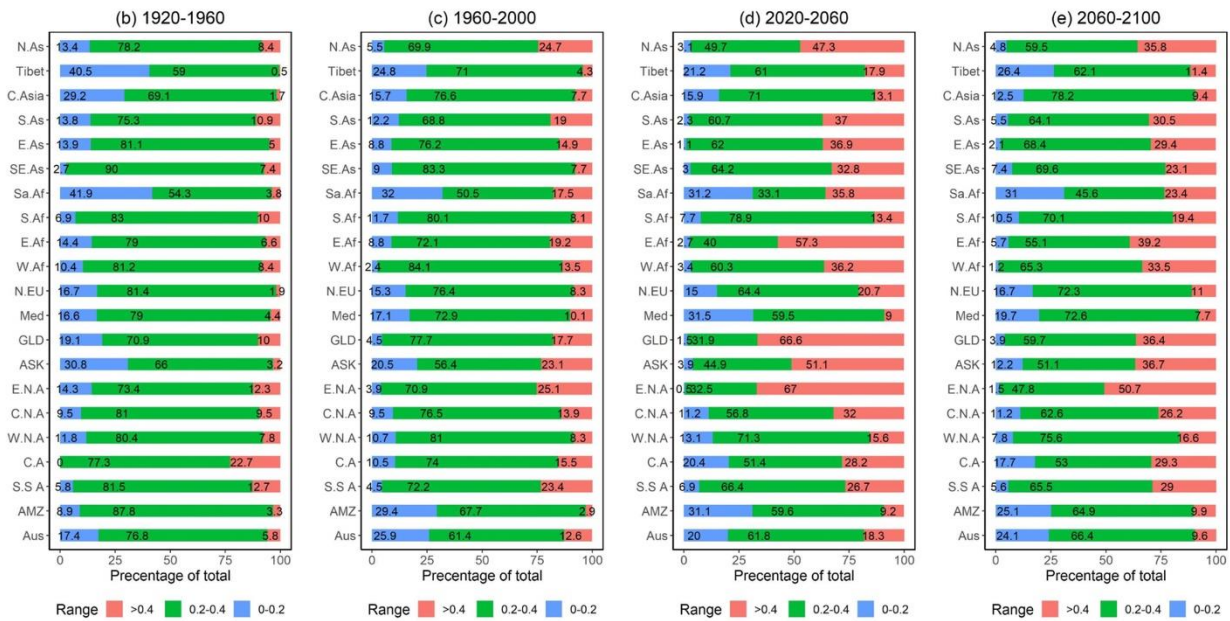
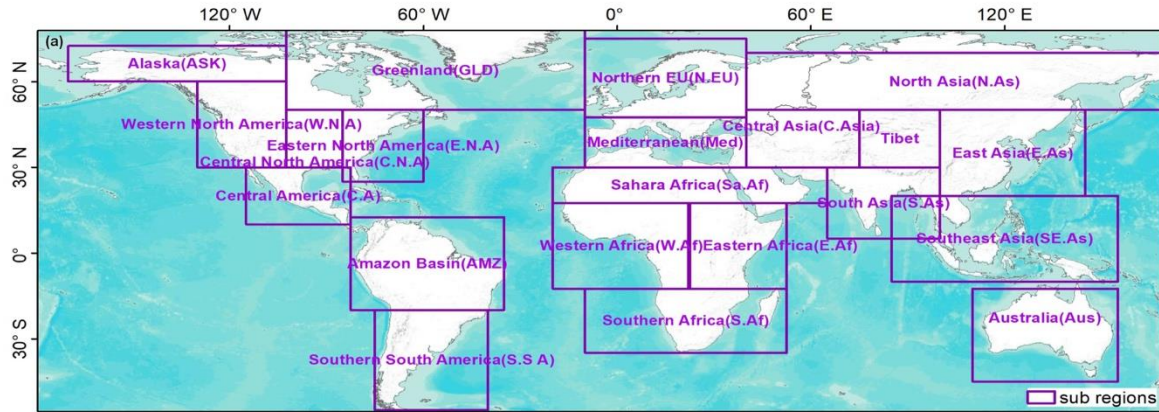
478

479 Figure 2. The percentage of global land areas subject to different levels of dry-to-wet transition  
 480 probabilities for 1920-1960 (a), 1960-2000 (b), 2020-2060 (c) and 2060-2100 (d).

481

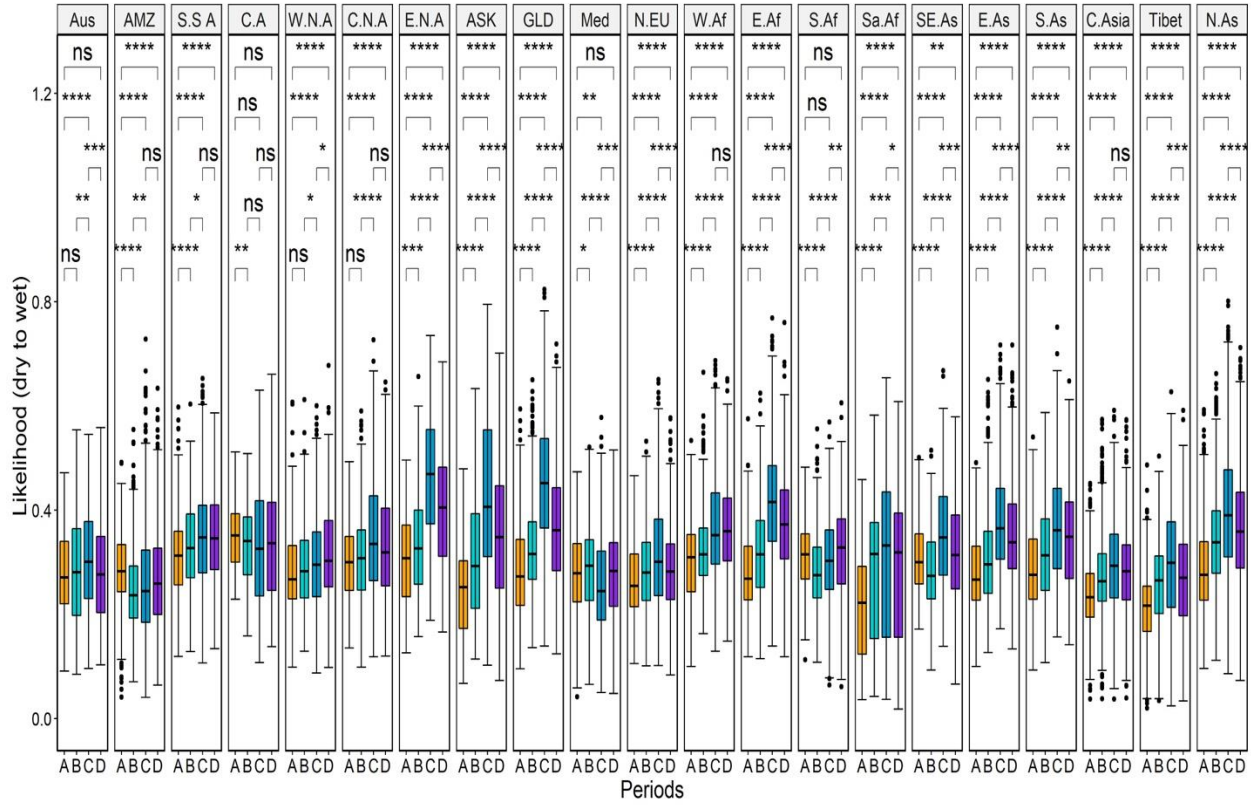
482

483



484  
485  
486  
487  
488  
489  
  
490  
491  
492

Figure 3. The percentage of global land areas subject to different levels of dry-to-wet transition probabilities for 21 subregions (a) during periods of 1920-1960 (b), 1960-2000 (c), 2020-2060 (c) and 2060-2100 (e).



493  
 494  
 495  
 496  
 497

Figure 4. The probability of transitioning from a significant drought year to a following extreme wet year during each of the four forty-year periods for the 21 subregions. A, B, C and D correspond to the periods of 1920-1960, 1960-2000, 2020-2060 and 2060-2100, respectively.

# Figures

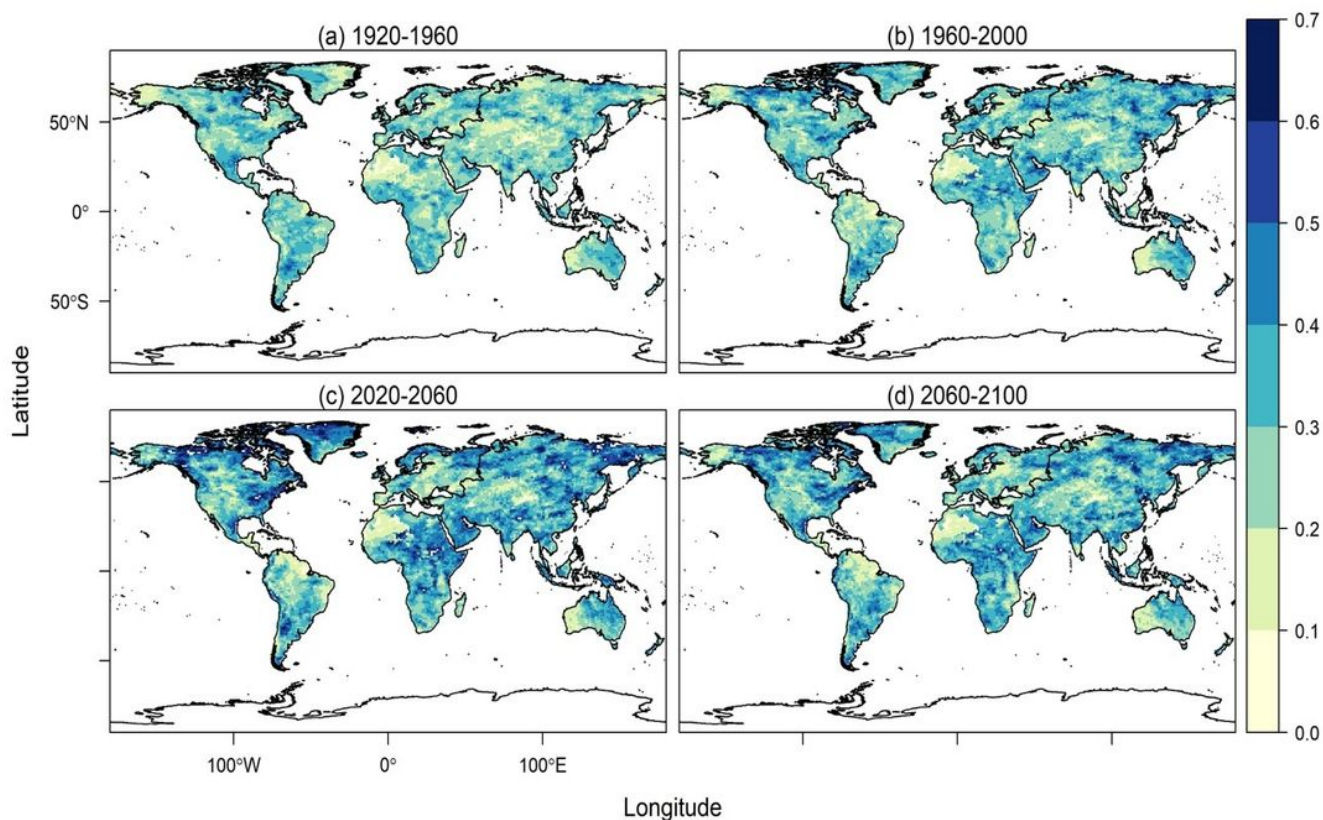


**Figure 1**

The probability of dry-to-wet precipitation events for four forty-year periods including 1920-1960 (a), 1960-2000 (b), 2020-2060 (c) and 2060-2100 (d). The dry-to-wet transition events are defined as the occurrence of two consecutive years during which the annual total precipitation falls under the 30th percentile of the baseline climatology (in the first year) and subsequently exceeds the 70th percentile of the same reference (in the following year). Note: The designations employed and the presentation of the material on this map do not imply the expression of any opinion whatsoever on the part of Research Square concerning the legal status of any country, territory, city or area or of its authorities, or concerning the delimitation of its frontiers or boundaries. This map has been provided by the authors.

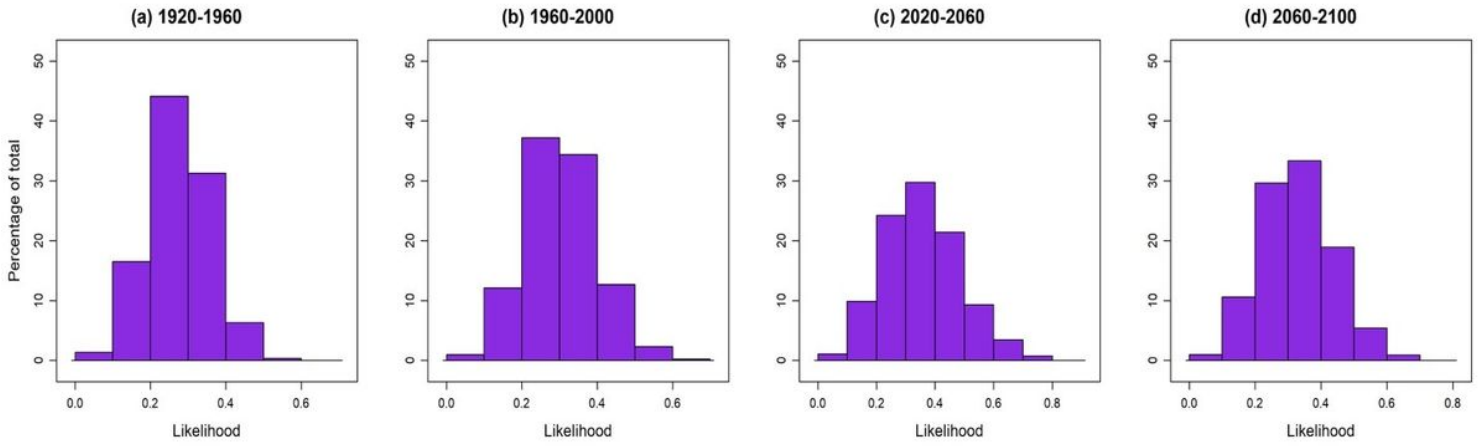


**Figure 2**

The percentage of global land areas subject to different levels of dry-to-wet transition probabilities for 1920-1960 (a), 1960-2000 (b), 2020-2060 (c) and 2060-2100 (d).

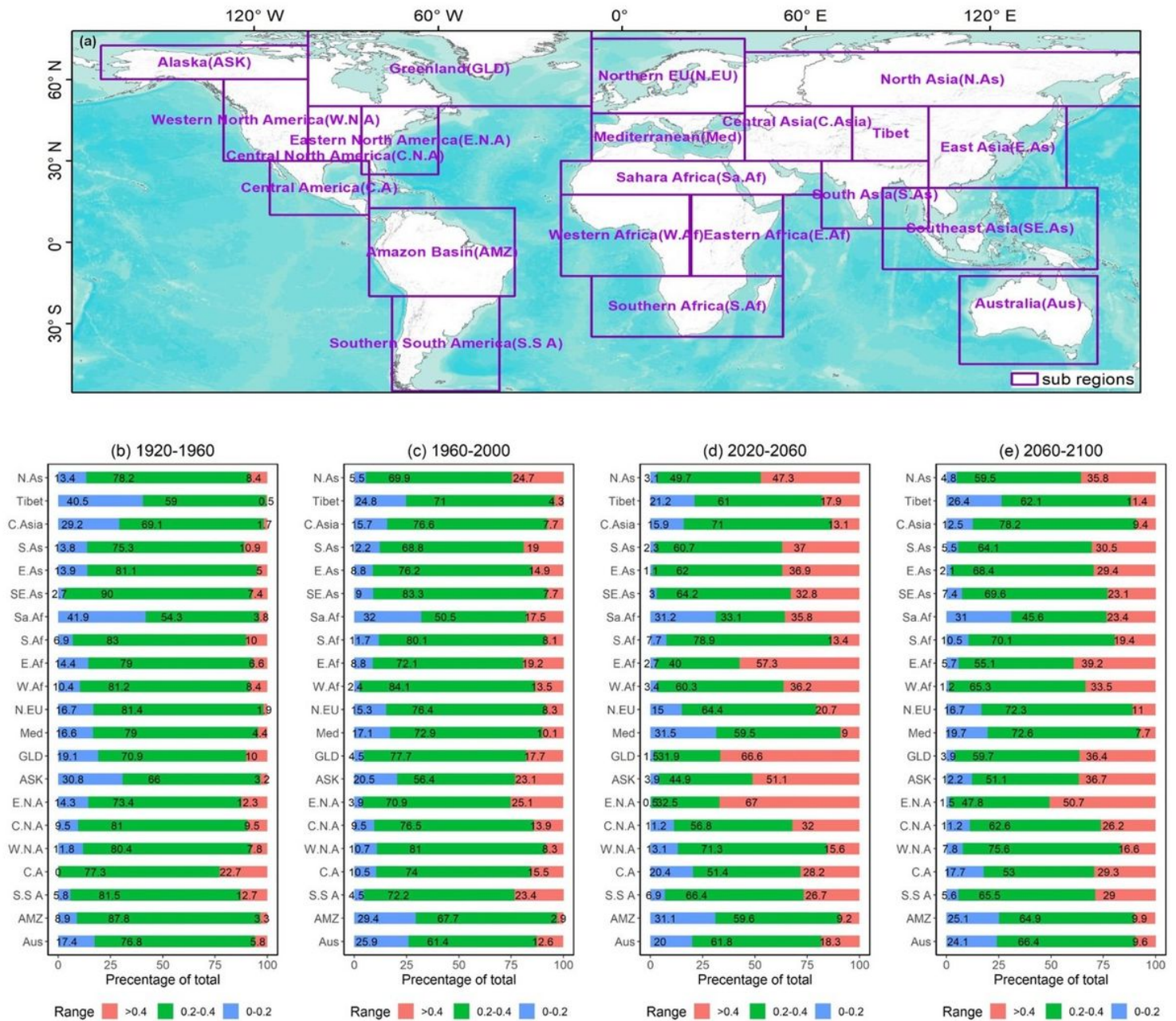


**Figure 3**

The percentage of global land areas subject to different levels of dry-to-wet transition probabilities for 21 subregions (a) during periods of 1920-1960 (b), 1960-2000 (c), 2020-2060 (c) and 2060-2100 (e). Note: The designations employed and the presentation of the material on this map do not imply the expression of any opinion whatsoever on the part of Research Square concerning the legal status of any country, territory, city or area or of its authorities, or concerning the delimitation of its frontiers or boundaries. This map has been provided by the authors.

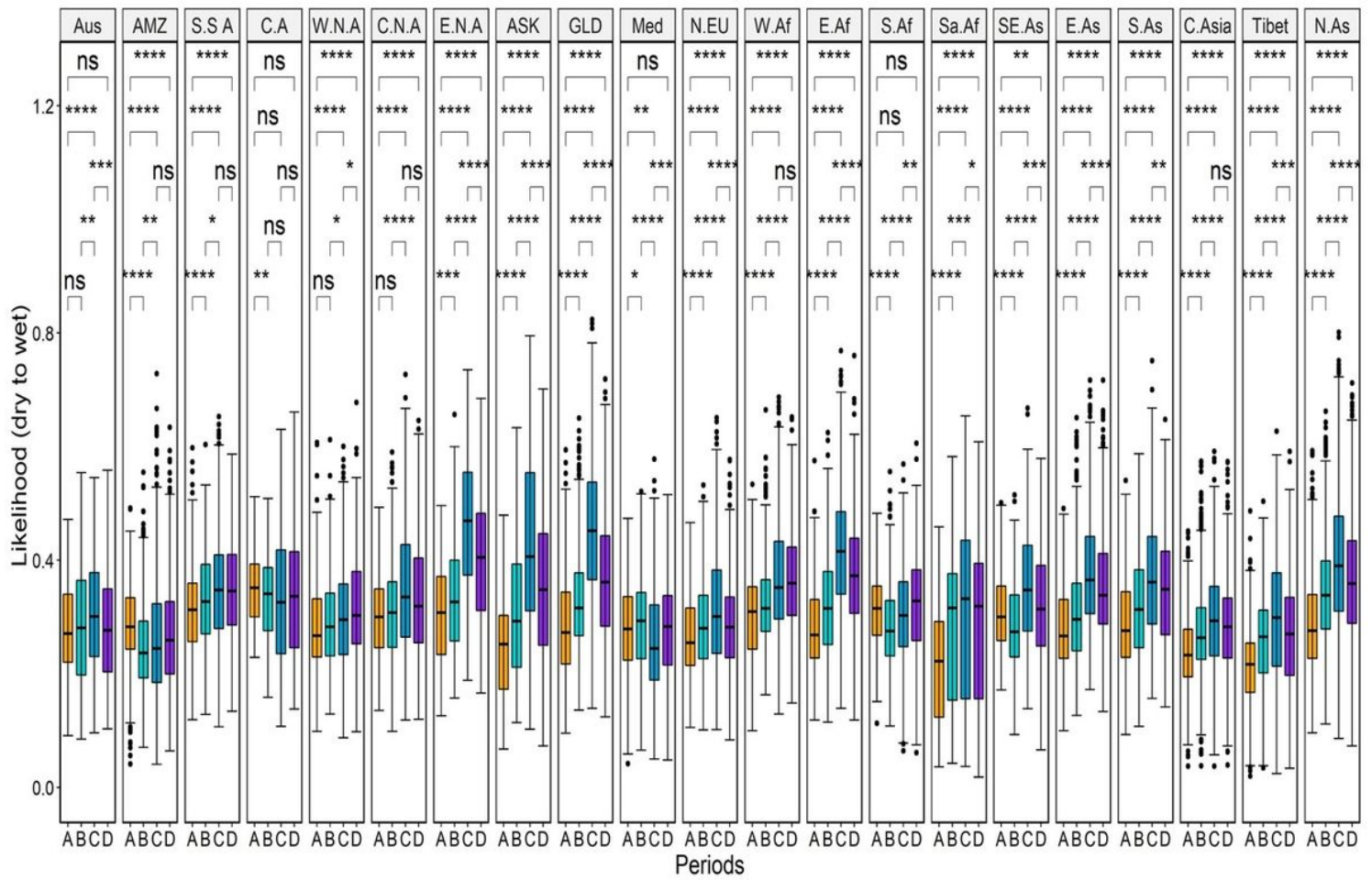


**Figure 4**

The probability of transitioning from a significant drought year to a following extreme wet year during each of the four forty-year periods for the 21 subregions. A, B, C and D correspond to the periods of 1920-1960, 1960-2000, 2020-2060 and 2060-2100, respectively.

## Supplementary Files

This is a list of supplementary files associated with this preprint. Click to download.

- [FigureS1.jpg](#)
- [FigureS2.jpg](#)
- [FigureS3.jpg](#)
- [FigureS4.jpg](#)